Carcinogenesis vol.32 no.3 pp.271–278, 2011
doi:10.1093/carcin/bgq253
Advance Access publication November 26, 2010

G-quadruplex structures in *TP53* intron 3: role in alternative splicing and in production of p53 mRNA isoforms

Virginie Marcel[1,7], Phong L.T.Tran[2], Charlotte Sagne[1,3], Ghyslaine Martel-Planche[1], Laurence Vaslin[3], Marie-Paule Teulade-Fichou[4], Janet Hall[3], Jean-Louis Mergny[2,5], Pierre Hainaut[1,*] and Eric Van Dyck[1,6]

[1]Group of Molecular Carcinogenesis, International Agency for Research on Cancer, 150 cours Albert Thomas, 69372, Lyon Cedex 08, France, [2]Muséum National d'Histoire Naturelle, INSERM U565, Centre National de la Recherche Scientifique UMR7196, 75231, Paris Cedex 05, France, [3]INSERM U612, Institut Curie-Recherche, 91405 Orsay, France, [4]Centre National de la Recherche Scientifique UMR176, Institut Curie-Recherche, 91405 Orsay, France, [5]INSERM U869, Institut Européen de Chimie Biologie, Université de Bordeaux, 33607 Pessac, France and [6]Laboratory of Experimental Hemato-Oncology, Public Center for Health (CRP-Santé), L-1526, Luxembourg, UK

[7]Present address: Department of Surgery and Molecular Oncology, INSERM-European Associated Laboratory, Ninewells Hospital and Medical School, Dundee, DD1 9SY, Scotland, UK

*To whom correspondence should be addressed. Tel: +33 4 72 73 84 62; Fax: +33 4 72 73 83 22;
Email: hainaut@iarc.fr

The tumor suppressor gene *TP53*, encoding p53, is expressed as several transcripts. The fully spliced p53 (FSp53) transcript encodes the canonical p53 protein. The alternatively spliced p53I2 transcript retains intron 2 and encodes Δ40p53 (or ΔNp53), an isoform lacking first 39 N-terminal residues corresponding to the main transactivation domain. We demonstrate the formation of *G-quadruplex* structures (G4) in a GC-rich region of intron 3 that modulates the splicing of intron 2. First, we show the formation of G4 in synthetic RNAs encompassing intron 3 sequences by ultraviolet melting, thermal difference spectra and circular dichroism spectroscopy. These observations are confirmed by detection of G4-induced reverse transcriptase elongation stops in synthetic RNA of intron 3. In this region, p53 pre-messenger RNA (mRNA) contains a succession of short exons (exons 2 and 3) and introns (introns 2 and 4) covering a total of 333 bp. Site-directed mutagenesis of G-tracts putatively involved in G4 formation decreased by ∼30% the excision of intron 2 in a green fluorescent protein-reporter splicing assay. Moreover, treatment of lymphoblastoid cells with 360A, a synthetic ligand that binds to single-strand G4 structures, increases the formation of FSp53 mRNA and decreases p53I2 mRNA expression. These results indicate that G4 structures in intron 3 regulate the splicing of intron 2, leading to differential expression of transcripts encoding distinct p53 isoforms.

Introduction

The tumor suppressor p53 protein controls antiproliferative responses to various forms of stress (1). Its function is impaired in >50% of human cancer, mainly by mutation (2). *TP53* gene expression is complex, with different transcripts encoding isoforms carrying distinct N- and C-termini (3,4). To date, 10 isoforms have been identified resulting from the usage of alternative promoters, splice sites and/or translational initiation sites (5). Several of these isoforms differ in their N-terminal region. The N-terminus of p53 contains the main transactivation domain (residues 1–42, transactivation domain I) as well as the binding site of Hdm2, which targets p53 for proteasome degradation and regulates p53 stability (1). Transcription of p53 messenger RNA (mRNA) from the proximal promoter generates two proteins with distinct N-terminal domain. The first corresponds to the canonical p53 protein, assembled from the fully spliced p53 (FSp53) mRNA that retains 11 exons. This protein induces p53-mediated growth suppression in response to stress. The second isoform, Δ40p53 (or ΔNp53), is assembled from an alternatively spliced mRNA retaining intron 2 (p53I2) and lacks the first 39 residues, corresponding to transactivation domain I, as well as Hdm2-binding site (3,6). The use of an internal promoter located in a region between intron 1 and exon 5 generates a third N-terminal isoform, Δ133p53, which lacks the first 132 residues (5).

When expressed in excess to p53, Δ40p53 inhibits transcriptional activity and interferes in the control of cell cycle progression and apoptosis by exerting a negative effect on the expression of p53-target genes (3,6,7). However, the biological circumstances and the molecular mechanisms regulating Δ40p53 expression are still poorly known. Retention of intron 2 in p53I2 mRNA introduces several stop codons in the reading frame of AUG 1, thus preventing the synthesis of a full-length p53 protein. However, p53I2 mRNA can be translated using AUG 40 as initiation site, generating a protein isoform which differs from the canonical p53 by the lack of the first 39 residues. Expression of p53I2 transcript has been reported in cell lines, such as MCF-7, in normal lymphocytes and in primary melanoma isolates (7,8). However, the mechanism that regulates the splicing of p53 pre-mRNA into FSp53 or p53I2 is not understood. Δ40p53 protein isoform can also be produced by internal ribosomal entry site-regulated internal initiation of translation using FSp53 mRNA (9,10).

In recent years, it has been proposed that tridimensional RNA structures such as *G-quadruplexes* may play important roles in regulating splicing (11). These structures result of the propensity of G-rich sequences to fold into four-stranded cation-dependent structures (12). They are formed by the interaction of four guanines organized in a cyclic Hoogsteen hydrogen bonding arrangement termed a G-quartet and by the stacking of several G-quartets (Figure 1A). It is estimated that over 376 000 sequences in the human genome have the potential to adopt *G-quadruplex* structures, most of them located in non-coding regions (13,14). At the RNA level, *G-quadruplexes* may play a number of roles. In non-coding RNAs, they can affect their structures and functions (15,16). In 5′-untranslated region of mRNAs, *G-quadruplexes* have been shown to modulate translation (17,18). When present in introns, *G-quadruplexes* can affect the splicing and expression patterns of genes such as *hTERT* (human telomerase reverse transcriptase), *Bcl-xL* or *FMRP* (Fragile X mental retardation protein) (11,19,20).

The sequence of intron 3 in *TP53* contains tracts of G bases organized in a pattern similar to the one of regions forming *G-quadruplex* structures. Since exon 3 in *TP53* is extremely short (22 bp), we reasoned that motifs located in intron 3 might have an effect on the regulation of the splicing of intron 2. In this study, we provide an evidence for the formation of *G-quadruplex* in *TP53* intron 3 and that these *G-quadruplex* structures may affect the splicing of intron 2, modulating the synthesis of either FSp53 (intron 2 spliced out) or p53I2 (intron 2 retained) mRNAs, which encode different p53 protein isoforms.

Materials and methods

Synthetic RNA oligomers and compounds

RNA oligomers derived from intron 3 of p53 RNA and containing several G-tracts (Figure 1B and C, Table I) were synthesized from IBA (Göttingen, Germany) at 0.2 μmol scale and resuspended in 20–40 μl of bidistilled water (ddH_2O). Concentrations of oligomers were determined by ultraviolet (UV) absorbance. The compound 360A [(2,6-N,N′-methyl-quinolinio-3-yl)-pyridine dicarboxamide] was stored in dimethyl sulfoxide and further diluted in ddH_2O for treating lymphoblastoid cell line for 48 h (21).

Abbreviations: CD, circular dichroism; FSp53, fully spliced p53; GFP, green fluorescent protein; mRNA, messenger RNA; PCR, polymerase chain reaction; RT, reverse transcriptase; TDS, thermal difference spectra; UV, ultraviolet.

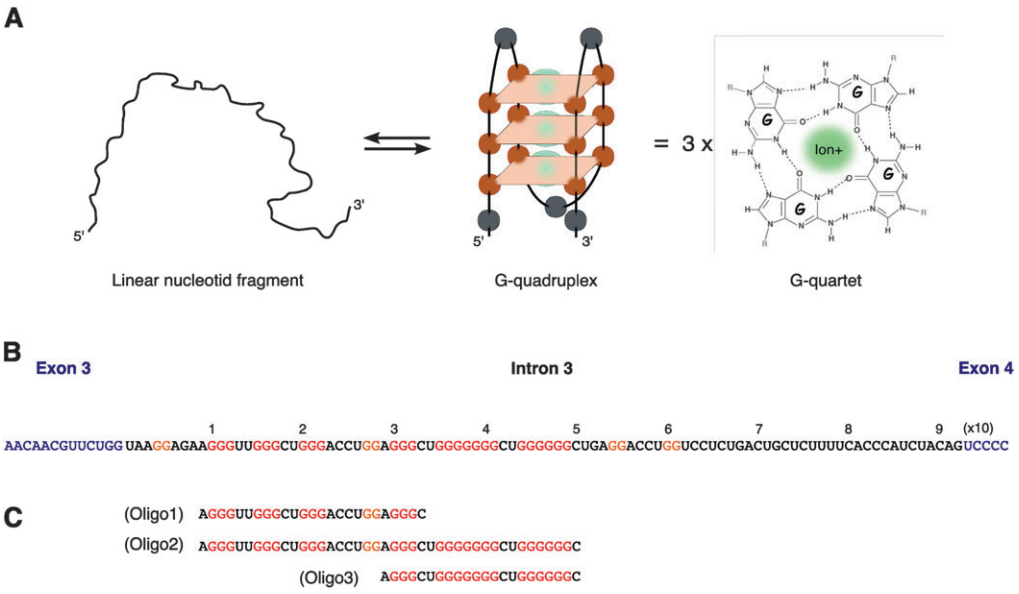

Fig. 1. Schematic representation of *G-quadruplex* and G-rich sequences in intron 3 of *TP53*. (**A**) Formation of *G-quadruplex* structure based on G-quartet element. Middle panel: tridimensional representation of a *G-quadruplex*; right panel: bidimensional representation of a G-quartet, stabilized by cations. (**B**) Partial sequence of *TP53* pre-mRNA from end of exon 3 to start of exon 4. Exonic sequences (blue), intronic sequences (black) and G-repeats (red and orange, three and two guanines, respectively) are shown. (**C**) Location and sequence of synthetic RNA oligomers 1, 2 and 3.

Table I. List of the oligomers used in this study

Oligomer name	Sequence (5′–3′)
Oligo1	AGGGUUGGGCUGGGACCUGGAGGGC
Oligo2	AGGGUUGGGCUGGGACCUGGAGGG-CUGGGGGGGCUGGGGGGC
Oligo3	AGGGCUGGGGGGGCUGGGGGGC
Oligo4	AGGGCUCACCACCCUCACCACC
RF16[a]	AAAAAAAAUUUUUUUU
RK50[a]	CGUAACGUUACG
G4-RNA 22 nts	AGGGUUAGGGUUAGGGUUAGGG
G4-RNA 46 nts	AGGGUUAGGGUUAGGGUUAGGGUUAGG-GUUAGGGUUAGGGUUAGGGG

[a]Self complementary RNA duplexes.

UV melting

The thermal stability of oligonucleotides was characterized in heating/cooling experiments by recording UV absorbance at 295 nm as a function of temperature using an Uvikon XL UV/Vis spectrophotometer (22). UV-melting experiments were conducted as described previously in 10 mM lithium cacodylate buffer, pH 7.2 containing either 100 mM LiCl, 100 mM NaCl or KCl at concentrations of 2 or 10 mM (23). Oligomers were tested at 3 μM strand concentration. The heating and cooling rates were 0.2°C/min. Experiments were performed in 1 cm path length quartz cuvettes.

UV thermal difference spectra

Thermal difference spectra (TDS) were obtained by difference between the absorbance spectra from unfolded (at high temperature, >90°C) and folded oligonucleotides (at low temperature, ~3°C). TDS provide specific signatures demonstrating *G-quadruplex* formation (24). Spectra were recorded between 220 and 330 nm at pH 7.0 in 100 mM NaCl in an Uvikon XL UV/Vis spectrophotometer using quartz cuvettes with an optical path length of 1 cm. RNA strand concentration was 3 M.

Circular dichroism spectroscopy

Circular dichroism (CD) spectra were recorded between 200 and 330 nm on a JASCO-810 spectropolarimeter as described previously (25). Spectra were recorded after heating/cooling experiment and at low temperature (>4°C). Oligomers were tested at 3 M strand concentration.

Fluorescence resonance energy transfer melting assay

The F21T oligonucleotide, mimicking human telomeric motifs and double-labeled with FAM and TAMRA at either end, was synthesized by Eurogentec (Seraing, Belgium) (Table I). Briefly, in the presence of 360A, this oligonucleotide folds into a stable *G-quadruplex*, thus allowing fluorescence transfer to occur. The melting of the F21T probe was recorded by measuring fluorescence emission as a function of temperature. Different unlabeled oligomers were used as competitors, including the *G-quadruplex*-forming Oligos 1, 2 and 3, the non-*G-quadruplex* forming Oligo4 and two negative control oligonucleotides which do not contain G-tracts (Table I) (26,27).

Reverse transcriptase elongation assay

Intron 3 RNA was synthesized by *in vitro* transcription with T7 RNA polymerase (Promega, Madison, WI) of a linearized pBSK plasmids containing intron 3. One microgram of pBSK, denatured in 0.2 N NaOH and 0.2 mM ethylenediaminetetraacetic acid (37°C 30 min), was sequenced using Sequenase T7 (Amersham, Pittsburgh, PA). Primer extensions were performed on 8 μmol of intron 3 RNA and 10^4 c.p.m. of ^{32}P-labeled BSK-R primer. Denaturation (95°C 1 min) and annealing (24°C 10 min) were completed in specific buffer (100 mM NaCl or KCl, 25 mM Tris–HCl pH 8.3, 10 mM $MgCl_2$ and 0.2 mM deoxynucleoside triphosphates) before extension (37°C, 30 min) using 30 U of AMV reverse transcriptase (RT) (Promega). Products were analyzed on 10% polyacrylamide–8 M urea gels following by autoradiography.

Green fluorescent protein-based reporter system

A PvuI restriction site was introduced into the pEGFP-N3 plasmid immediately after the first ATG of green fluorescent protein (GFP) to produce the GFP-Pos plasmid. A negative control plasmid was produced by Klenow fragment digestion at PvuI site. A fragment from exon 2 to exon 4 of *TP53* gene, excluding ATG 1 and 40, was cloned into the PvuI restriction site of GFP-Pos plasmid. Mutant GFP-Δ and GFP-ΔΔ plasmids were produced by QuickChange® site-directed Mutagenesis Kit (Stratagene, Santa Clara, CA) (supplementary Table I available at *Carcinogenesis* Online). In six-well plates, 5×10^5 of H1299 p53-null cells were transfected with 0.2 μg/ml of these plasmids using Fugene (Roche, Basel, Switzerland), RNA expression was analyzed by reverse transcription–polymerase chain reaction (PCR) (supplementary Table IIis available at *Carcinogenesis* Online), whereas GFP protein fluorescence was analyzed by flow cytometry.

Real-time PCR analysis

A lymphoblastoid cell line (BC9) expressing wild-type p53 and derived from breast cancer patient was used (28). Total RNA was extracted using Trizol Reagent (Invitrogen™, Carlsbad, CA). The level of each N-terminal variant p53 mRNA was analyzed using QuantiTect™ Syber® Green PCR Kit (Qiagen, Hamburg, Germany) and specific primers (supplementary Table I available at *Carcinogenesis* Online and Figure 5B) and normalized to that of glycerAldehyde 3-phosphate dehydrogenase. The Δ*C*t was calculated as an average of three measurements by plate for two quantitative reverse transcription–PCR of at least two independent experiments.

Statistical analyses

Analysis of variance and Student's *t*-tests were performed using online tools (http://faculty.vassar.edu/lowry/VassarStats.html).

Results

G-quadruplex structures in intron 3 of p53 mRNA

TP53 intron 3 (93 bp) is rich in G bases (41%). To analyze whether this *TP53* region may contain motifs capable of forming *G-quadruplex*, the prediction software Quadfinder server and the web-based server QGRS Mapper were used (29,30). Using default parameters to predict *G-quadruplex* motifs over the whole gene sequence, four candidate regions were identified: two regions in intron 1, one in intron 3 and another in intron 6 (data for intron 3 in supplementary Figure 1A and Bis available at *Carcinogenesis* Online; data for other introns not shown). The predicted *G-quadruplex*-forming motif in intron 3 was located 60 bp downstream of the splice acceptor site of intron 2 (supplementary Figure 1A and Bis available at *Carcinogenesis* Online). This motif is predicted to carry up to 5 G-tracts sequences capable of forming *G-quadruplex* structures (supplementary Figure 1A and Bis available at *Carcinogenesis* Online).

To demonstrate the formation of *G-quadruplex* structures in *TP53* intron 3, we synthesized three RNA oligomers derived from the G-rich region of intron 3 (Figure 1C, Table I) and we analyzed their thermal stability under different ionic conditions by UV melting (Figure 2A). For each of the three oligomers, the highest melting temperatures (T_m) were observed in K^+ (10 mM) buffer (Oligo1: 57°C; Oligo2: 66.5°C and Oligo3: 75°C). T_m was dependent on the nature of the cation, with T_m (Li^+ 100 mM) < T_m (Na^+ 100 mM) < T_m (K^+ 10 mM). This dependence is typical of the effect of these cations on the stability of *G-quadruplexes*. The T_m values of Oligo2 and 3 in K^+ 10 mM (66.5°C and 75°C, respectively) were higher than for Oligo1 (57°C), suggesting that *G-quadruplexes* in Oligo2 and 3 were more stable than in Oligo1. Oligo2 and 3 differ from Oligo1 by the presence of two tracts of six guanines in their 3′ domain (Figure 1C), suggesting that these G-repeats are important for stable G-quadruplex formation.

To further demonstrate the presence of G4, we used two different biophysical methods. First, we analyzed the profiles of the three oligomers using UV TDS (Figure 2B) and CD spectroscopy (Figure 2C). A TDS is obtained by recording the UV absorbance spectra of the unfolded and folded states at temperatures above and below the melting temperature (T_m). The TDS profiles of the three oligomers showed a positive peak at 273 nm and a negative peak at 295 nm (Figure 2B). These two peaks are typical 'signatures' of *G-quadruplex* structures as determined by the analysis of different types of *G-quadruplexes* (24). The variations in TDS profiles are independent of oligomer concentrations but reflect differences in sequence and in stability of G4. In particular, the low amplitude of the peaks observed with Oligo3 may be due to the fact that in this Oligo3, *G-quadruplex* structures are stable and only undergo partial unfolding within the temperature interval. CD spectroscopy also displayed changes in ellipticity, a characteristic of *G-quadruplex* structures, including a negative peak at 240 nm and a positive peak at 260 nm (Figure 2C). Overall, these results

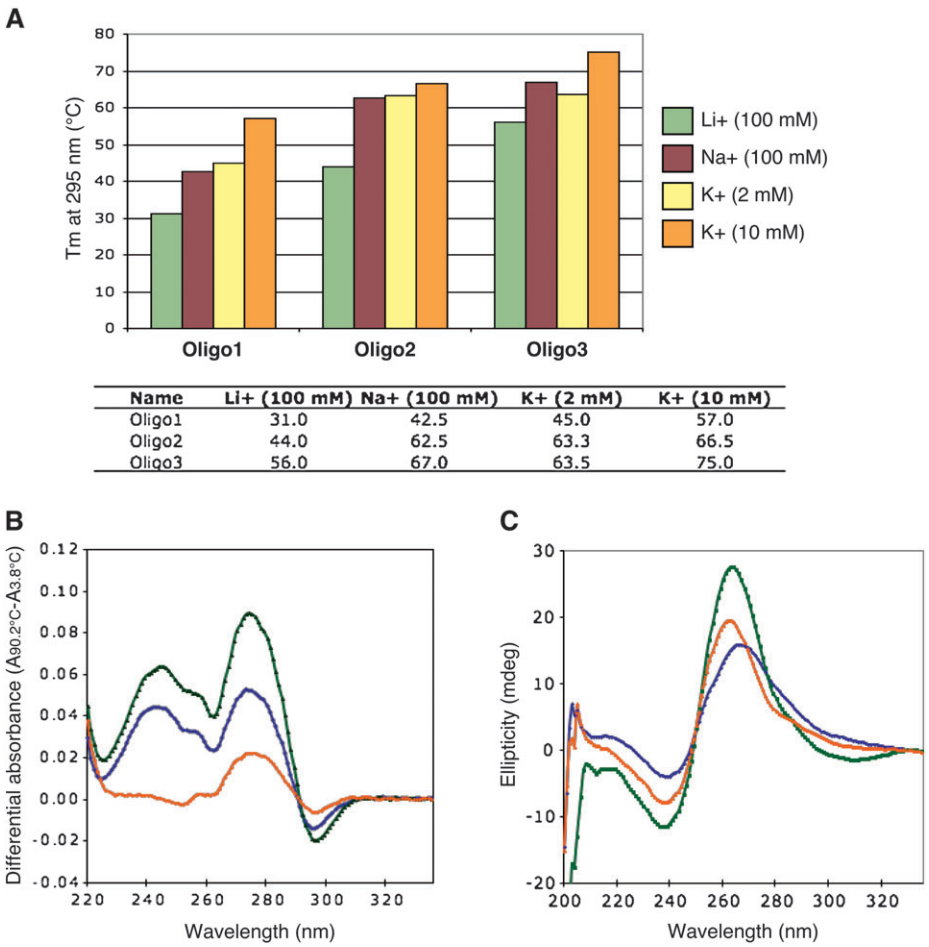

Name	Li+ (100 mM)	Na+ (100 mM)	K+ (2 mM)	K+ (10 mM)
Oligo1	31.0	42.5	45.0	57.0
Oligo2	44.0	62.5	63.3	66.5
Oligo3	56.0	67.0	63.5	75.0

Fig. 2. Detection of *G-quadruplex* structures in synthetic RNA by spectroscopic methods. (**A**) UV melting experiments. Histograms (upper panel) and values (lower panel) of melting temperatures (T_m) ± 1°C at 295 nm for Oligo1–3 in different ionic conditions. (**B**) TDS of Oligos 1–3. Blue: Oligo1; green: Oligo2; Red: Oligo3. Presence of a positive peak at 273 nm and a negative peak at 295 nm are characteristic signatures of *G-quadruplexes* (24). (**C**) CD spectra of Oligo1–3 at 4°C in 10 mM KCl. Blue: Oligo1; green: Oligo2; red: Oligo3.

using synthetic RNA confirm *in silico* predictions and provide evidence that *G-quadruplex* structures can be formed in intron 3 of p53 RNA, involving in particular two G-repeats of six guanines.

Detection of G-quadruplexes by RT elongation assay

Next, we used the RT elongation assay to further identify the position of guanines involved in *G-quadruplexes* (Figure 3). This method takes advantage of the differential cation-dependent stability of *G-quadruplexes* to identify structures that interfere with RT elongation (31). K^+ stabilizes *G-quadruplexes*, leading to a K^+-dependent block of complementary DNA synthesis at positions where guanines are involved in a G-quartet. In contrast, in the presence of Na^+, *G-quadruplex* stability is reduced, allowing complementary DNA synthesis to proceed without elongation block. A full-length RT product corresponding to the entire intron 3 RNA was detected in presence of Na^+ (lane 5, '5′-intron 3' arrow in Figure 3). However, in the presence of K^+, stops of RT elongation were observed (lane 6) at positions corresponding to guanines on sequencing analysis, matching those predicted to form the 3′ end of the *G-quadruplexes*. Thus, the detection of several RT-stops is compatible with *in silico* prediction and with spectrometric analyses indicating a critical role of two tracts of six guanines in the formation of several *quadruplex* conformers in intron 3.

Role of G-quadruplex in excision of intron 2 using an in vitro splicing assay

Because alternative splicing of *TP53* involves either retention (p53I2) or skipping (FSp53) of intron 2, we examined whether *G-quadruplex*

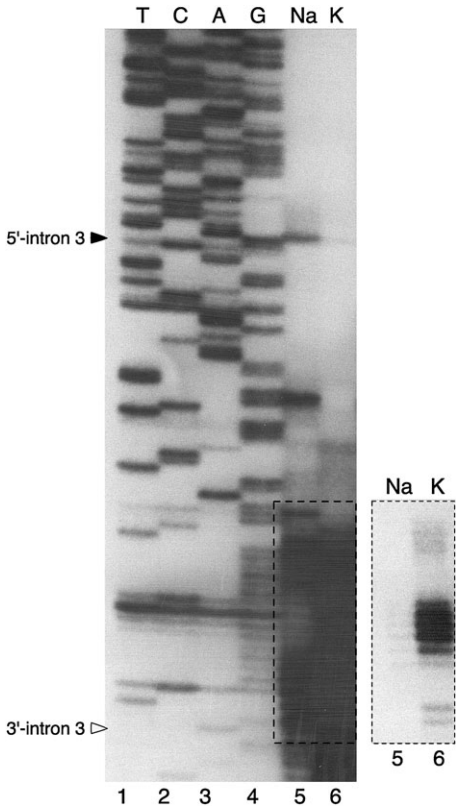

Fig. 3. RT elongation assay identifying RT-stops at guanines involved in *G-quadruplexes*. *G-quadruplexes* were mapped by reverse transcription of intron 3 sequences with a radiolabeled oligonucleotide in the presence of either Na^+ (destabilizing G4) or K^+ (stabilizing G4) and products were separated by denaturing gel electrophoresis (lanes 5–6). Lanes 1–4: dideoxy sequencing of the sequence used for reverse transcription. RT-stops (lanes 5–6) occurred at guanines residues as shown by comparison with the sequencing lanes. Black arrowhead: 5′-intron 3 end; open arrowhead: 3′-intron 3 end; Box on the right: short exposure of the area delimited by dotted lines, identifying the presence of strong stops at defined guanines in lane 6.

in intron 3 were involved in the regulation of this splicing. To analyze the direct effect of *G-quadruplexes* on the splicing of intron 2, we constructed a minigene reporter based on GFP, in which a *TP53* fragment from exons 2 to 4 was cloned between the ATG and the GFP coding sequence (GFP-E2E4, Figure 4A). With this construct, correct splicing of intron 2 (FS–GFP) produces an mRNA that supports GFP synthesis, whereas retention of intron 2 (I2-GFP) introduces stop codons preventing GFP expression. Two mutant versions of the reporter were constructed, in which either one (GFP-E2E4Δ) or both (GFP-E2E4ΔΔ) two tracts of six guanines predicted to be involved in *G-quadruplexes* were substituted by site-directed mutagenesis (Figure 4B). To verify that the mutations introduced in GFP-E2E4ΔΔ abolished *G-quadruplex* formation, we synthesized an RNA oligomer, Oligo4, containing the same mutations (Figure 4B and Table I). When compared with Oligo2 and 3, Oligo4 did not show the typical patterns of *G-quadruplexes* detected by UV-melting curves, TDS and CD spectra (supplementary Figure 1A and Bis available at *Carcinogenesis* Online).

The p53-null cell line H1299 were transfected with the various GFP constructs. All constructs displayed equal transfection efficiency, as determined by reverse transcription–PCR analysis of expression of the *neomycin* gene carried by the plasmids (Figure 4C). When compared with cells expressing the wild-type GFP-E2E4 construct, cells transfected with GFP-E2E4Δ and -E2E4ΔΔ showed an increase in I2-GFP mRNA expression (retaining intron 2) and a decrease of FS–GFP mRNA expression (correct splice-out of intron 2). GFP fluorescence measurements showed that the wild-type GFP-E2E4 construct generated as much fluorescence as the positive GFP control (GFP-pos) (Figure 4). Mutation of guanines resulted in a progressive decrease in fluorescence that depended upon the number of guanines mutated. A significant reduction of fluorescence of ∼25% was observed when comparing GFP-E2E4ΔΔ with GFP-E2E4 ($P < 0.05$). Taken together, these observations support the hypothesis that *G-quadruplexes* in intron 3 modulate the rate at which intron 2 is spliced-out. With wild-type intron 3 sequences presumably capable of forming stable *G-quadruplexes*, splicing of intron 2 appears to be more efficient than when *G-quadruplex* formation is crippled by mutations.

Effects of G-quadruplexes on p53 splicing in lymphoblastoid cells

To determine whether *G-quadruplexes* may modulate the splicing of p53 in intact cells, we analyzed the effect of a specific ligand of *G-quadruplex* structures, 360A, on the expression of FSp53 and p53I2 transcripts in lymphoblastoid cells using real-time PCR (Figure 5). The ligand 360A has high affinity and stabilizing effects for *G-quadruplex* structures in single-stranded nucleic acids (21). To demonstrate that 360A could bind to *G-quadruplexes* in intron 3 of p53 RNA, we used an fluorescence resonance energy transfer melting assay (Figure 4A) (27). A DNA oligonucleotide mimicking human telomeric motifs (F21T) was labeled with FAM at the 5′ end and TAMRA at the 3′ end (26,27). Addition of 360A induced a concentration-dependent stabilization of the *G-quadruplex*, resulting in an increased melting temperature (ΔT_m), at which fluorescence emission ceases due to unfolding of the *G-quadruplex* that suppresses fluorescence transfer. Excess amounts of unlabeled DNA or RNA were used as competitors to determine their capacity to displace 360A from its fluorescent target, thereby reducing its melting temperature. Figure 5A shows that Oligo1, 2 and 3 were capable of acting as competitors, in contrast with mutant Oligo4 and with negative control sequences RF16 and RK50. These results indicate that RNA *quadruplexes* formed in *TP53* intron 3 could bind 360A, further extending the sequence repertoire of G4 structures bound by this ligand.

We next treated human lymphoblastoid cell line with 50 nM 360A for 48 h and analyzed its effects on p53 mRNA expression (Figure 5B and C). Although 360A did not exert significant toxicity at the concentrations used (supplementary Figure 3 available at *Carcinogenesis* Online), it induced opposite, dose-dependent effects on levels of the two p53 transcripts, FSp53 and p53I2 (Figure 5C). Treatment by 360A resulted in a significant 3-fold increase in FSp53 mRNA.

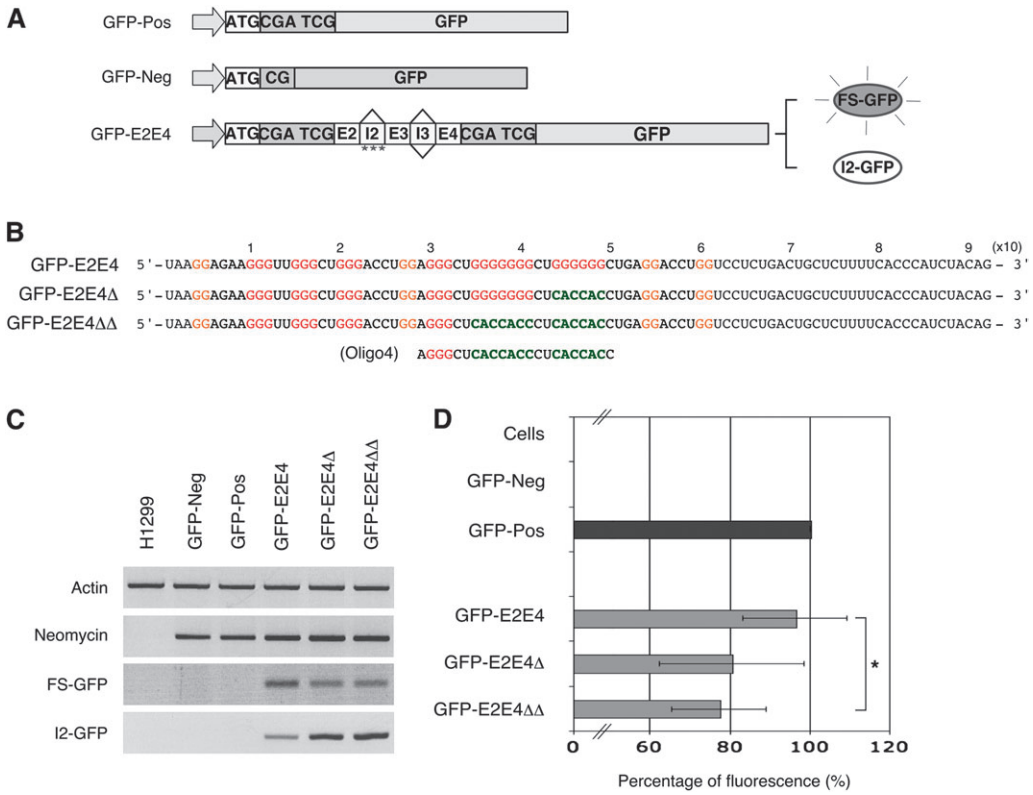

Fig. 4. GFP reporter splicing assay to analyze the role of *G-quadruplexes* in alternative splicing of intron 2. (**A**) Schematic representation of constructs used in the GFP-based reporter system. A fragment from exon 2 to exon 4, excluding both ATG 1 and 40, was cloned into the GFP-Pos plasmid (serving as positive control) to construct the GFP-E2E4 reporter. With this reporter, GFP fluorescence is generated only after correct excision of intron 2 since the latter contains stop codons that preclude protein synthesis from ATG1 (asterisks). Arrow: CMV promoter and Kozak sequence. (**B**) Mutations disrupting *G-quadruplexes* in GFP-E2E4 reporter. Guanines involved in *G-quadruplexes* were mutated (green letters). The synthetic RNA Oligo4 was designed to verify by spectroscopic methods that mutation of these guanines prevented the formation of *G-quadruplexes* (see supplementary Figure 1, available at *Carcinogenesis* Online). (**C**) mRNA expression analysis of GFP-E2E4, Δ and ΔΔ mutants. Constructs were transfected in H1299 cells and their expression was analyzed by semiquantitative reverse transcription–PCR and agarose gel electrophoresis. As compared with GFP-E2E4, a decrease in fully spliced mRNA (FS–GFP) and an increase of intron 2 retaining mRNA (I2-GFP) were observed. Actin: loading control; neomycin: control of transfection efficiency. (**D**) Analysis of GFP fluorescence of transfected H1299 by flow cytometry. Compared with GFP-Pos GFP-E2E4, Δ and ΔΔ mutants exhibited a decrease of GFP fluorescence, indicating an increase of intron 2 retention. $^{*}P < 0.05$; Student's *t*-test based on duplicate of five independent experiments.

In contrast, p53I2 levels were significantly decreased by ∼40%. These results support the notion that *G-quadruplexes* are involved in the regulation of intron 2 splicing in intact cells.

Discussion

TP53 is expressed as several isoforms produced by different mechanisms, including alternative splicing (4,7). Differential splicing of intron 2 leads to the generation of FSp53 and p53I2 mRNAs that respectively encode the tumor suppressor p53 and the Δ40p53 isoform, which lacks the transactivation domain and acts as a negative regulator of p53 activity (7,32). Therefore, mechanisms that control the alternative splicing of intron 2 may have an effect on p53 activity by modifying the relative expression levels of p53 and of its Δ40p53 isoform. In this study, we show that a region of intron 3 forming *G-quadruplex* structures in p53 pre-mRNA is involved in the alternative splicing of *TP53* intron 2. First, we used synthetic RNAs containing sequences of intron 3 and we show that these RNA can form *G-quadruplexes* using different spectrometric methods (UV melting, TDS and CD spectroscopy). Next, the presence of *G-quadruplexes* is further demonstrated by RT elongation assays. In these assays, demonstration of a *G-quadruplex* relies on the fact that these structures are very dependent upon the presence of specific cations, being stabilized in the presence of K^+ and destabilized in the presence of Na^+. Furthermore, to demonstrate the involvement of these *G-quadruplex* structures in the splicing of intron 2, we have constructed a GFP reporter system in which fluorescence emission is dependent upon the correct excision of intron 2 sequences. Using this system, we show that mutation of guanines involved in *G-quadruplexes* significantly decreases the splicing-out of intron 2, however, without abolishing it. Finally, to demonstrate that *G-quadruplexes* in intron 3 can impact on p53 splicing in intact cells, we used a novel pharmacological ligand that stabilizes *G-quadruplexes*, 360A, in lymphoblastoid cells and we show that treatment with this ligand induces significant changes in the expression patterns of FSp53 (encoding p53) and p53I2 (encoding Δ40p53) mRNAs. Specifically, 360A increased the levels of FSp53 mRNA and decreased the ones of p53I2 mRNA, consistent with studies using the GFP reporter system showing that presence of stable *G-quadruplexes* is important for efficient splicing-out of intron 2.

The notion that *G-quadruplex* structures can modulate the alternative splicing of several genes is not new: it has been demonstrated in the case of β-tropomyosin, hTERT or Bcl-xL transcripts (11,19,33). Compared with these examples, p53 *G-quadruplexes* show two important features. First, they are located in another intron (intron 3) than the one affected by alternative splicing (intron 2). This particular topography is due to the fact that introns and exons in this region are extremely short and some of the regulatory signals for the splicing of this intron may actually be located in intron 3. The splice acceptor of intron 2 is located just 60 bp upstream of the sequence forming *G-quadruplexes*. Second, the effects we demonstrate here are only partial. They do not induce a complete shift from one splicing pattern to the other, but rather modify the equilibrium between the two

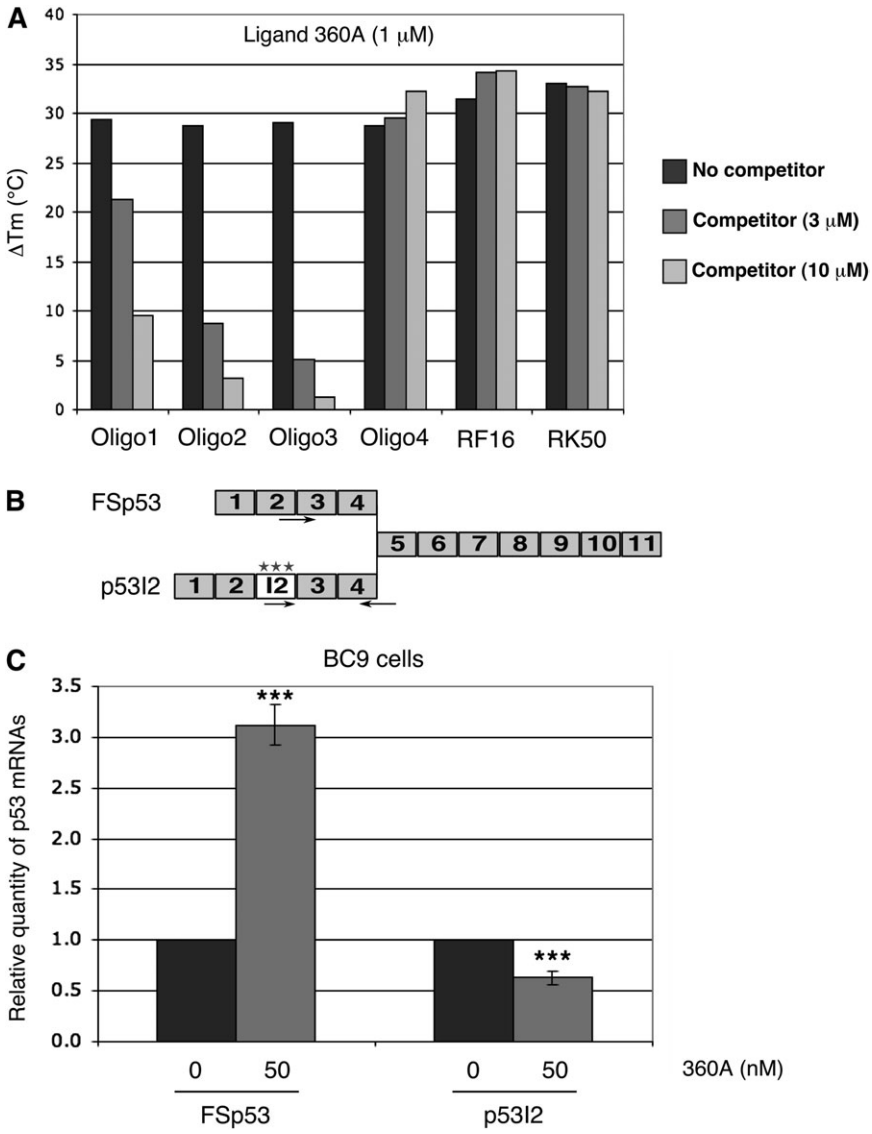

Fig. 5. Effect of the *G-quadruplex* ligand 360A on expression of p53 transcripts. (**A**) fluorescence resonance energy transfer assay demonstrating the capacity of 360A to bind intron 3 *G-quadruplexes*. The ΔT_m values for an oligonucleotide forming a canonical *G-quadruplex* (derived from *hTERT* sequence) were calculated in the presence or in the absence of competing oligonucleotides Oligo1–4 or control double-stranded RNAs (RF16 and RK50). (**B**) Structure of alternative p53 transcripts and positions of primers for quantitative reverse transcription–PCR. The FSp53 mRNA includes exons 1 to 11 and produces p53. The p53I2 mRNA retains intron 2 (I2) but correctly splices out all other introns. Asterisks: stop codons in intron 2; arrows: primers used for real-time PCR. (**C**) Quantitative reverse transcription–PCR analysis of mRNA isolated from BC9 lymphoblastoid cells using Sybr Green. Cells were treated for 48 h with 50 nM of 360A and levels of FSp53 and p53I2 were measured. $^{***}P < 0.001$; Student's *t*-test based on duplicate of five independent experiments.

spliced products in a subtle manner. Using the GFP reporter system, the shift in splicing patterns observed after mutagenesis of candidate guanines is ~25% ($P < 0.05$). In lymphoblastoid cells treated with 360A, we detect significant changes in the levels of both transcripts ($P < 0.001$), with a 3-fold increase for FSp53 and a 40% decrease for p53I2. These observations may be due, at least in part, to the fact that *G-quadruplexes* in intron 3 are polymorphic and may exist as different conformers. It is therefore possible that our site-directed mutagenesis experiments do not completely remove all *G-quadruplex* structures along the sequence of intron 3 but merely displace them or modify their organization. Furthermore studies will be necessary to uncover the full extent of the effect of *G-quadruplexes* on the splicing of intron 2.

The biological consequences of the regulatory effects identified here remain to be determined. Changes in transcript levels are expected to result into changes in the expression of both p53 protein isoforms when *G-quadruplexes* are stabilized, leading to increased p53 expression and decreased Δ40p53 expression. Indeed, we observed that 360A treatment resulted in a slight increased of p53 protein expression but we did not detect any significant impact on Δ40p53 protein levels or on the expression of the p53-target gene $p21^{WAF1}$ (supplementary Figure 4 available at *Carcinogenesis* Online). This suggests that 360A ligand modulates p53 splicing but that this effect does without significant activation of p53. Although p53 has a short half-life due to rapid recognition and proteasome-dependent degradation by Hdm2, Δ40p53 escapes this regulation and is much more stable (3,6). Furthermore, the biological effect of Δ40p53 remains controversial. Biochemical evidence shows that Δ40p53 interacts with p53 protein to form hetero-tetramers and that excess amounts of Δ40p53 downregulate the transactivation capacity of p53. When cotransfected together with wild-type p53 in p53-null cells, Δ40p53 prevents growth suppression by p53 and enhances clonogenicity (3,5,11,34). However, there is no evidence from *in vivo* studies that Δ40p53 operates as a suppressor of p53 function. In mice

with wild-type p53, increased dosage of Δ40p53 by expression of a transgene leads to accelerate aging and short lifespan. These mice display cognitive decline and synaptic impairment early in life, attributed to hyperactivation of insulin-like growth factor 1 receptor signaling and altered metabolism of the microtubule-binding protein tau (35,36). In human cells, Δ40p53 has been implicated in G_2 cell cycle arrest in response to endoplasmic reticulum stress (37). Although the molecular mechanisms of these effects are not understood, both mouse and human models suggest that small variations of Δ40p53 are sufficient to modify p53 biological function.

Another important consideration with respect to the potential impact of *G-quadruplex* in intron 3 is that they include guanine residues that are part of a common polymorphism, *TP53* PIN3, consisting of a 16 bp duplication (rs17878362; A1: non-duplicated allele; A2: duplicated allele) (38,39). Several epidemiological case–control studies have identified that the carriers of the A2 allele had a significantly increased risk of several common cancers, including breast, colorectal, lung and ovarian cancers (28,40–42). Recently, we have reported that *TP53* PIN3 is a genetic modifier of germ line *TP53* mutation in the Li-Fraumeni Syndrome, the A1 allele being associated with earlier age at first cancer diagnosis (43). Interestingly, Gemigniani *et al.* (28) described that p53 mRNA levels were lower in lymphoblastoid cell lines with A2 than with A1 alleles, suggesting that this polymorphism may affect the levels of p53 transcripts. *In silico* models predicts that *TP53* PIN3 may alter the topology of *G-quadruplexes* in intron 3 (data not shown). However, the extent of these modifications and their consequences on p53 splicing remains to be investigated.

In conclusion, our results demonstrate that *G-quadruplexes* are present in intron 3 of *TP53* gene and provide support in favor of a role of these structures in the regulation of the alternative splicing of intron 2, thus modulating the patterns of expression of transcripts encoding either p53 or its N-terminally truncated isoform, Δ40p53.

Supplementary material

Supplementary Tables I and II and Figures 1–4 can be found at http://carcin.oxfordjournals.org/

Funding

This work is supported by INSERM, Institut National contre le Cancer (INCa, France, Projet Libre 2009, 2009-192), an Agence Nationale de la Recherche grant (G4-toolbox), the Région Aquitaine (J.-L.M.) and by la Ligue Contre le Cancer (France), including a fellowship from La Ligue Nationale to V.M.

Acknowledgements

The authors thank Dr Hervé Moine for initial help in identifying candidate sequences forming *G-quadruplexes*.

Conflict of Interest Statement: None declared.

References

1. Vousden,K.H. *et al*. (2007) p53 in health and disease. *Nat. Rev. Mol. Cell Biol.*, **8**, 275–283.
2. Petitjean,A. *et al*. (2007) Impact of mutant p53 functional properties on TP53 mutation patterns and tumor phenotype: lessons from recent developments in the IARC TP53 database. *Hum. Mutat.*, **28**, 622–629.
3. Courtois,S. *et al*. (2002) DeltaN-p53, a natural isoform of p53 lacking the first transactivation domain, counteracts growth suppression by wild-type p53. *Oncogene*, **21**, 6722–6728.
4. Bourdon,J.C. *et al*. (2005) p53 isoforms can regulate p53 transcriptional activity. *Genes Dev.*, **19**, 2122–2137.
5. Marcel,V. *et al*. (2009) p53 isoforms—a conspiracy to kidnap p53 tumor suppressor activity? *Cell. Mol. Life Sci.*, **66**, 391–406.
6. Yin,Y. *et al*. (2002) p53 Stability and activity is regulated by Mdm2-mediated induction of alternative p53 translation products. *Nat. Cell Biol.*, **4**, 462–467.
7. Ghosh,A. *et al*. (2004) Regulation of human p53 activity and cell localization by alternative splicing. *Mol. Cell. Biol.*, **24**, 7987–7997.
8. Avery-Kiejda,K.A. *et al*. (2008) Small molecular weight variants of p53 are expressed in human melanoma cells and are induced by the DNA-damaging agent cisplatin. *Clin. Cancer Res.*, **14**, 1659–1668.
9. Candeias,M.M. *et al*. (2006) Expression of p53 and p53/47 are controlled by alternative mechanisms of messenger RNA translation initiation. *Oncogene*, **25**, 6936–6947.
10. Ray,P.S. *et al*. (2006) Two internal ribosome entry sites mediate the translation of p53 isoforms. *EMBO Rep.*, **7**, 404–410.
11. Gomez,D. *et al*. (2004) Telomerase downregulation induced by the G-quadruplex ligand 12459 in A549 cells is mediated by hTERT RNA alternative splicing. *Nucleic Acids Res.*, **32**, 371–379.
12. Lipps,H.J. *et al*. (2009) G-quadruplex structures: *in vivo* evidence and function. *Trends Cell Biol.*, **19**, 414–422.
13. Huppert,J.L. *et al*. (2005) Prevalence of quadruplexes in the human genome. *Nucleic Acids Res.*, **33**, 2908–2916.
14. Todd,A.K. *et al*. (2005) Highly prevalent putative quadruplex sequence motifs in human DNA. *Nucleic Acids Res.*, **33**, 2901–2907.
15. Henn,A. *et al*. (2008) Inhibition of dicing of guanosine-rich shRNAs by quadruplex-binding compounds. *Chembiochem*, **9**, 2722–2729.
16. Gros,J. *et al*. (2008) G-quadruplex formation interferes with P1 helix formation in the RNA component of telomerase hTERC. *Chembiochem*, **9**, 2075–2079.
17. Kumari,S. *et al*. (2007) An RNA G-quadruplex in the 5' UTR of the NRAS proto-oncogene modulates translation. *Nat. Chem. Biol.*, **3**, 218–221.
18. Wieland,M. *et al*. (2007) RNA quadruplex-based modulation of gene expression. *Chem. Biol.*, **14**, 757–763.
19. Didiot,M.C. *et al*. (2008) The G-quartet containing FMRP binding site in FMR1 mRNA is a potent exonic splicing enhancer. *Nucleic Acids Res.*, **36**, 4902–4912.
20. Hai,Y. *et al*. (2008) A G-tract element in apoptotic agents-induced alternative splicing. *Nucleic Acids Res.*, **36**, 3320–3331.
21. Granotier,C. *et al*. (2005) Preferential binding of a G-quadruplex ligand to human chromosome ends. *Nucleic Acids Res.*, **33**, 4182–4190.
22. Mergny,J.L. *et al*. (1998) Following G-quartet formation by UV-spectroscopy. *FEBS Lett.*, **435**, 74–78.
23. Mergny,J.L. *et al*. (2003) Analysis of thermal melting curves. *Oligonucleotides*, **13**, 515–537.
24. Mergny,J.L. *et al*. (2005) Thermal difference spectra: a specific signature for nucleic acid structures. *Nucleic Acids Res.*, **33**, e138.
25. Guedin,A. *et al*. (2008) Sequence effects in single-base loops for quadruplexes. *Biochimie*, **90**, 686–696.
26. Mergny,J.L. *et al*. (2001) Fluorescence resonance energy transfer as a probe for G-quartet formation by a telomeric repeat. *Chembiochem*, **2**, 124–132.
27. De Cian,A. *et al*. (2007) Fluorescence-based melting assays for studying quadruplex ligands. *Methods*, **42**, 183–195.
28. Gemignani,F. *et al*. (2004) A TP53 polymorphism is associated with increased risk of colorectal cancer and with reduced levels of TP53 mRNA. *Oncogene*, **23**, 1954–1956.
29. Kikin,O. *et al*. (2006) QGRS Mapper: a web-based server for predicting G-quadruplexes in nucleotide sequences. *Nucleic Acids Res.*, **34**, W676–W682.
30. Scaria,V. *et al*. (2006) Quadfinder: server for identification and analysis of quadruplex-forming motifs in nucleotide sequences. *Nucleic Acids Res.*, **34**, W683–W685.
31. Weitzmann,M.N. *et al*. (1996) The development and use of a DNA polymerase arrest assay for the evaluation of parameters affecting intrastrand tetraplex formation. *J. Biol. Chem.*, **271**, 20958–20964.
32. Matlashewski,G. *et al*. (1987) Alternative splicing of human p53 transcripts. *Oncogene Res.*, **1**, 77–85.
33. Sirand-Pugnet,P. *et al*. (1995) An intronic (A/U)GGG repeat enhances the splicing of an alternative intron of the chicken beta-tropomyosin pre-mRNA. *Nucleic Acids Res.*, **23**, 3501–3507.
34. Powell,D.J. *et al*. (2008) Stress-dependent changes in the properties of p53 complexes by the alternative translation product p53/47. *Cell Cycle*, **7**, 950–959.
35. Maier,B. *et al*. (2004) Modulation of mammalian life span by the short isoform of p53. *Genes Dev.*, **18**, 306–319.
36. Pehar,M. *et al*. (2010) Altered longevity-assurance activity of p53:p44 in the mouse causes memory loss, neurodegeneration and premature death. *Aging Cell*, **9**, 174–190.
37. Bourougaa,K. *et al*. (2010) Endoplasmic reticulum stress induces G2 cell-cycle arrest via mRNA translation of the p53 isoform p53/47. *Mol. Cell.*, **38**, 78–88.
38. Lazar,V. *et al*. (1993) Simple sequence repeat polymorphism within the p53 gene. *Oncogene*, **8**, 1703–1705.

39. Runnebaum,I.B. *et al*. (1994) Multiplex PCR screening detects small p53 deletions and insertions in human ovarian cancer cell lines. *Hum. Genet.*, **93**, 620–624.
40. Hung,R.J. *et al*. (2006) Sequence variants in cell cycle control pathway, X-ray exposure, and lung cancer risk: a multicenter case-control study in Central Europe. *Cancer Res.*, **66**, 8280–8286.
41. Runnebaum,I.B. *et al*. (1995) p53-based blood test for p53PIN3 and risk for sporadic ovarian cancer. *Lancet*, **345**, 994.
42. Wang-Gohrke,S. *et al*. (2002) Intron 3 16 bp duplication polymorphism of p53 is associated with an increased risk for breast cancer by the age of 50 years. *Pharmacogenetics*, **12**, 269–272.
43. Marcel,V. *et al*. (2009) TP53 PIN3 and MDM2 SNP309 polymorphisms as genetic modifiers in the Li-Fraumeni syndrome: impact on age at first diagnosis. *J. Med. Genet.*, **46**, 766–772.

Received August 2, 2010; revised November 5, 2010; accepted November 14, 2010